SEMARAK ILMU PUBLISHING

Journal of Advanced Research in Applied Sciences and Engineering Technology

Journal homepage:
https://semarakilmu.com.my/journals/index.php/applied_sciences_eng_tech/index
ISSN: 2462-1943

Delamination Assessment via Acoustic Wave Propagation and an Optical Sensor Network

Ihsan Naiman Ibrahim[1], Mohd Hafizi Zohari[1,*], Mohd Fadhlan Mohd Yusof[1], Gigih Priyandoko[2]

[1] Advanced Structural Integrity and Vibration Research (ASIVR), Faculty of Mechanical and Automotive Engineering Technology, University Malaysia Pahang Al-Sultan Abdullah (UMPSA), 26600 Pekan, Pahang, Malaysia
[2] Dept of Electrical Engineering, Faculty of Engineering, University of Widyagama Malang, Indonesia

ARTICLE INFO

Keywords:

Fiber Bragg grating (FBG) sensor; acoustic waves propagation; delamination; structural health monitoring (SHM)

ABSTRACT

The preservation of the integrity of composite structures necessitates the monitoring of their structural health. A considerable body of research has been dedicated to investigating the use of traditional electrical sensors for the purpose of collecting acoustic waves in order to detect delamination. In contrast, electrical sensors possess several limitations. This research endeavors to evaluate delamination by employing an optical sensor network that relies on a fiber Bragg grating (FBG) sensor. In the experiment, composite plates were fabricated with varying sizes of delamination. The composite specimen has been equipped with a sensor network consisting of four Fiber Bragg Gratings (FBGs) placed linearly. This network enables the detection of acoustic wave propagation resulting from an impact in the middle of the composite plate. Upon analysis of the acoustic waves, it is seen that the average time delay for various delamination circumstances is 68.2% for a delamination size of 10 cm x 4 cm and 116.7% for a delamination size of 10 cm x 6 cm. The findings of the study also demonstrate that the reduction in wave speed is 40.54% and 53.85% for delamination sizes of 10 cm x 4 cm and 10 cm x 6 cm, respectively. The results indicate that the utilization of a network of Fiber Bragg Grating (FBG) sensors for the purpose of delamination detection in plate-like composite structures holds promise in the field of health monitoring.

1. Introduction

Composite materials are advantageous due to their superior mechanical performance, high thermal resistance, good fire behavior, high impact resistance, best abrasion resistance, extraordinary electrical insulation, and rigidity [1]. Moreover, a composite made from natural fiber has a long lifespan and can support rehabilitation efforts, making it a cost-effective and environmentally responsible option for extending the life of structures and reducing their carbon dioxide footprint [2]. Composite structures are frequently susceptible to barely visible impact damage (BVID), such as delamination, throughout extended periods of operation [3-5]. Hence, it is

* *Corresponding author.*
E-mail address: hafizi@umpsa.edu.my

https://doi.org/10.37934/araset.63.4.93104

imperative to implement structural health monitoring (SHM) techniques to avoid the spread of delamination and mitigate the degradation of structural integrity in composite structures.

The failure mechanism of composite structures, such as carbon fiber reinforced plastic (CFRP) laminates, when subjected to static or dynamic loads, is characterized by distinct microscopic damages, including matrix fractures and delamination. Delamination, for instance, can result in a decrease in stiffness and frequently culminates in catastrophic collapse. This research explores the complex dynamics of delamination in Carbon Fiber-Reinforced Polymer composites during Vibration Assisted Trimming, using an examination of historical data. The analysis investigates various elements, including processing parameters, material qualities, and environmental circumstances, in order to reveal valuable insights that are essential for increasing the trimming process and improving the durability of composite production [6]. The evaluation of delamination detection has significant importance in engineering applications, as it serves as a crucial factor in assessing the dependability of composite laminates [7]. The detection of delamination by the propagation of acoustic waves is well documented in academic literature.

An acoustic wave refers to a type of mechanical wave that arises from the vibration produced by a specific source. Longitudinal waves, shear waves, Rayleigh waves, and Lamb waves are considered as acoustic wave phenomena [8]. Lamb waves are frequently created within a thin-walled construction, which facilitates the evaluation of internal defects via the thickness [9]. The sensitivity of lamb waves and their coda waves to disbond size and interface position has been confirmed by an experimental study conducted on a honeycomb sandwich composite plate extracted from the Airbus A330 lift. This study demonstrates the feasibility of detecting disbonds using data taken from a single side [10]. Meanwhile, Jagadeeshwar *et al.,* [11] suggested a baseline-free technique that relies on statistics and ultrasonic guided waves to quickly analyze delamination in composite structures. This approach was then confirmed using experimental data, demonstrating a strong level of agreement. In addition, Xu *et al.,* [12] introduced a novel Lamb wave imaging technique that utilizes weighted sparse decomposition coefficients and the minimum variance distortionless response algorithm. This method aims to identify anomalies or damage in laminated composite plates. Experimental findings on a quasi-isotropic laminated composite plate validate the efficacy of this approach.

Throughout the course of time, acoustic emission (AE) sensors and piezoelectric transducers (PZT) have been widely acknowledged as the standard sensors employed for the purpose of catching acoustic waves. The study conducted by Wang *et al.,* [13] examined the application of piezoelectric composite material as both structural components and sensing elements for the analysis of guided wave propagation and interaction with damage. The findings indicated that the utilization of piezoelectric composite material showed significant promise in the implementation of Structural Health Monitoring (SHM). The use of multiple piezoelectric transducers (PZTs) for monitoring the delamination of composite double cantilever beams was described by Zhao *et al.,* [14]. The signals obtained from the piezoelectric transducers (PZTs) were subjected to post-processing techniques including the Hilbert transform, Fourier transforms, and wavelet transform. The findings of the study indicate that variations in delamination length have a significant impact on both the timing of arrival and the higher frequency modes.

In their study, Hervin *et al.,* [15] employed the use of PZT (lead zirconate titanate) to examine the phenomenon of Lamb wave mode scattering on a composite structure that had delaminations. The findings indicated a substantial correlation between the depth of delamination and the amplitude of the waves. In their study, Aggelis *et al.,* [16] affixed a total of eight acoustic emission (AE) sensors onto a hybrid cement material that was reinforced with a composite hollow beam. The purpose of this setup was to observe and track the occurrence of matrix cracking and delamination inside the material. The findings of the study indicated that the occurrence of matrix cracking was associated

with elevated frequency values, whereas the presence of delamination was linked to decreased frequency values. Li *et al.,* [17] employed two acoustic emission (AE) sensors to examine the impact of delamination length in a composite cantilever beam on the rising angle and strain energy release rate of the waveforms. The findings indicated that both criteria have demonstrated efficacy in the detection of delamination. Saeedifar *et al.,* [18] employed acoustic emission (AE) sensors for the purpose of analysing the delamination behaviour in laminated composite constructions.

In this study, two composite specimens underwent indentation loading. The waveforms obtained from the acoustic emission (AE) sensors were evaluated using the b-value and sentry function techniques. The findings of the study indicate that Acoustic Emission (AE) proved to be an effective sensor for the detection and assessment of BVID in laminated composites. However, it is worth noting that all the aforementioned investigations utilized traditional electrical sensors. Electrical sensors are frequently accompanied by a range of drawbacks, including significant signal attenuation, susceptibility to electromagnetic interference (EMI), and unsuitability for operation in challenging environmental conditions [19,20]. The aforementioned limitations can be effectively addressed by the utilisation of fibre optic sensors. Fibre Bragg grating (FBG) sensors have been extensively studied and widely published in the field of fibre optic sensors because of its numerous advantages. These advantages include their compact size, immunity to electromagnetic interference (EMI), and suitability for operation in hostile environments [21-23].

The field of research focused on using Fibre Bragg Grating (FBG) sensing for the purpose of detecting delamination is currently limited in scope. The observed phenomenon can be attributed to the presence of heterogeneous and unequal strain fields generated by the growth of delamination cracks. These strain fields lead to the occurrence of several peaks in the reflected spectral response of the Fibre Bragg Gratings (FBGs), making their interpretation complex and lacking a straightforward method. In order to address this issue, a number of studies have employed sensors with short gauge lengths or affixed the sensors directly onto the surface of the specimen [24,25]. Previous studies conducted deliberate placement of Fibre Bragg Grating (FBG) sensors inside a strain field that exhibited non-uniform characteristics [26-28]. Nevertheless, the reflection spectrum of Fibre Bragg Grating (FBG) alone is insufficient for accurately determining the position and direction of delamination development. This limitation arises from the mixed shape of the reflection spectrum, which is induced by the presence of a nonhomogeneous strain field in the vicinity of the delamination. The limitations were mitigated by the use of FBG sensors as dynamic sensors for the acquisition of acoustic waves. In their study, Takahashi *et al.,* [29] found that an acoustic sensor utilizing a Fiber Bragg Grating (FBG) exhibits comparable or superior performance to a traditional Piezoelectric (PZT) acoustic sensor in terms of many fundamental characteristics, including sensitivity, linearity, frequency response, and compactness. Meanwhile, Gong *et al.,* [30] conducted experiments to demonstrate the high sensitivity of their proposed FBG acoustic sensing system. Their findings indicated that the system is capable of detecting ultrasonic waves within the frequency range of hundreds of kilohertz. This suggests that the system has promise for practical applications in the field of acoustic emission detection. When appropriately packaged, strain sensors with consistent, high sensitivity and linear characteristics can be advantageous for various applications that require the detection of seismic vibrations, underwater acoustic signals, low amplitude accelerations, and similar scenarios [31].

This study focuses on the analysis of signal parameters of acoustic waves in order to enhance the reliability of delamination growth detection using a network of Fiber Bragg Grating (FBG) sensors. FBG sensors have the capability to be affixed to the surfaces of pre-existing structures and may also be included into newly constructed structures during the fabrication process without compromising their structural integrity. Ultimately, the resultant signal emanating from the Structural Health

Monitoring (SHM) system has the potential to provide an advanced indication of the integrity of the structure, therefore mitigating substantial losses and averting catastrophic collapses.

2. Methodology

Two delaminated composite plates were fabricated with the hand lay-up method. Each specimen is made up of four fiberglass layers. The fiberglass sheets were arranged as chopped strand mat (CSM) 450 with 0° orientation, woven roving 300 with 90° orientation, woven roving 300 with 45° orientation and CSM 450 with -45°. Reversal P-9509 NW was used as the resin and Butanox M-60 methyl ethyl ketone peroxide (MEKP) was used as the curing agent.

The composite plates have the following dimensions: 90 cm in length, 90 cm in breadth, and 0.3 cm in thickness as shown in Figure 1. Each composite plate has four FBG sensors surface-bonded to it, as shown in Figure 1(b). All FBGs were arranged to form a sensor network in straight line. The FBG sensor is made up of a brief segment of Bragg grating that reflects the Bragg wavelength (λ_B), which is represented by the following Eq. (1):

$$\lambda_B = 2\eta_e \Lambda \tag{1}$$

where η_e is the effective refractive index and λ is the grating period. The Bragg wavelength shifts are temperature and strain sensitive which can be denoted as:

$$\frac{\Delta\lambda}{\lambda_B} = (\hat{a} + \mathcal{E})\Delta T + (1 - p_e)\varepsilon \tag{2}$$

where $\Delta\lambda$ is the change in the wavelength, $\hat{a}$ is the thermal expansion, $\mathcal{E}$ is the thermo-optic coefficient, ΔT is the change in temperature, p_e is the effective photo-elastic constant of the fiber, and ε is the strain induced. This experimentation was carried out in a temperature-controlled environment where the change in temperature can be neglected and the expression can be simplified as:

$$\frac{\Delta\lambda}{\lambda_B} = (1 - p_e)\varepsilon \tag{3}$$

Therefore, for an acoustic wave travelling on the specimen, the amplitude of the wave can be related to the changes of Bragg wavelength (λ_B) as it is linearly correlated to the dynamic strain induced by the waves.

At 15 cm from the centre of each specimen, a delamination was artificially created. CSM 450 and tissue mat were inserted into the intermediate layer of the fiberglass to create the delamination. The size of the delamination for the first composite structure is 10 cm x 4 cm, which referring to width (W) x length (L). Meanwhile the delamination area for the second composite structure is 10 cm x 6 cm. Since the FBGs were arranged in one dimensional (1D) and the detection area is between the FBG 3 and FBG 4, the delamination size also can be referred to the ratio between the length of FBG 3 to FBG 4 ($L_{FBG4-FBG3}$) and the length (W) of the delamination area:

$$\text{Delamination size } (\%) = \frac{L_{FBG4-FBG3}}{W} \times 100 \tag{4}$$

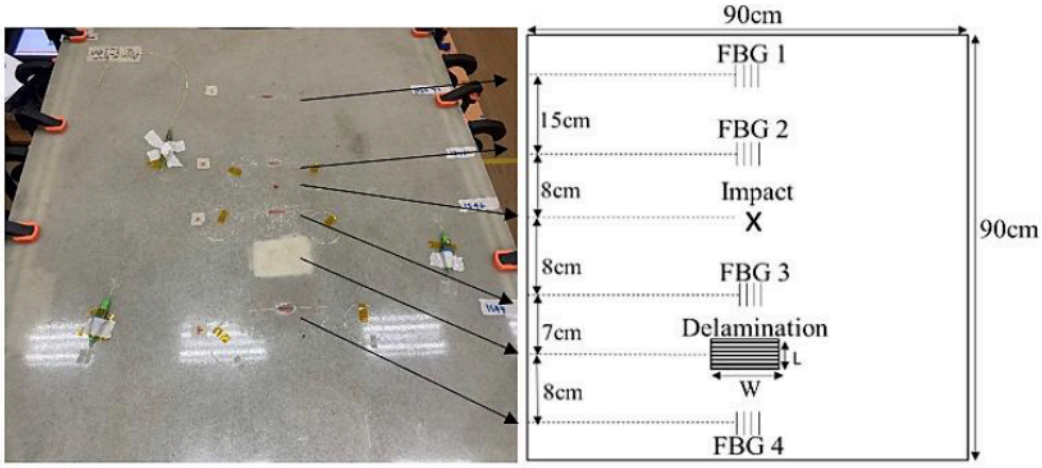

(a) (b)

Fig. 1. The fabricated specimen (a) Photo of the composite structure (b) Illustration of the composite structure

The composite plate was clamped at eight positions, as illustrated in Figure 2. During the experimentation, the broadband light from the light source (LS) was distributed to all the FBG sensors via optical circulator in multiplexed connection. The reflected light signals from all FBGs were then channeled to the FBG interrogator (OSA). All data was post processed using a computer. Note that, for assessment of delamination size 10 cm x 4 cm and 10 cm x 6 cm, the FBG sensor network was arranged vertically. Meanwhile, for the case of no delamination, the FBG sensors network was installed horizontally where there is no delamination through the detection line, as shown in Figure 3. However, the orientation of the sensor, whether it is vertical or horizontal, is not anticipated to have an impact on the signal detected by the FBG sensors. The reason is that the composite specimen possesses symmetrical geometry, measuring 90cm x 90cm, and also exhibits symmetrical fiber glass layer orientation.

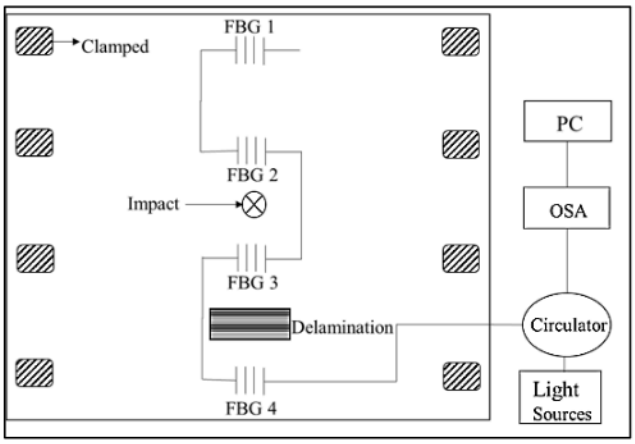

Fig. 2. Illustration of the experimental setup for assessment of delamination size 10 cm x 4 cm and 10 cm x 6 cm

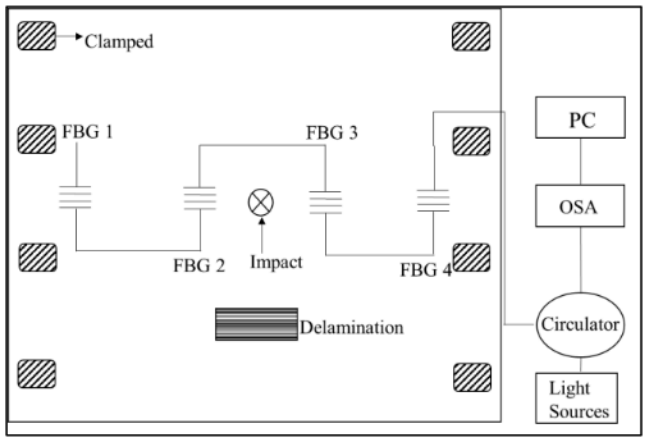

Fig. 3. Illustration of the experimental setup for assessment of no delamination with horizontal FBG layout

Initial values for all FBGs on all specimens were recorded prior to the data collection, at room temperature of 26.8°C. To initiate the acoustic waves, an impact was done at the centre of the specimen. Ten impact trials were induced for each delamination condition of the specimen, for better repeatability. These procedures were first performed on a specimen area without delamination, followed by specimen with delamination area of 10 cm × 4 cm and 10 cm × 6 cm. The

waveforms captured by FBG 1, FBG 2, FBG 3 and FBG 4 were then analyzed for time delay analysis and its velocity comparison.

3. Results and Discussion

3.1 Time Delay Analysis

Figures 4, 5, and 6 show the time arrival variation of the acoustic wave between FBG 1 and FBG 2 (ΔT_{2-1}); and FBG 3 and FBG 4 (ΔT_{4-3}), for sensing areas without delamination and delamination areas of 10 cm × 4 cm and 10 cm × 6 cm, respectively. Sensors FBG 2 and FBG 3 were positioned near the impact; therefore, the waveform will be first captured by FBG 2 and FBG 3, followed by FBG 1 and FBG 4. Due to this, a time arrival difference between both waveforms can be observed and analyzed. To calculate the time difference, an arbitrary peak was selected for both signals for comparison. For instance, consider the sensor network (FBG 1–4) without delamination; as shown in Figure 4, a peak of the waveform for FBG 1 was recorded at 1464.0 ms, whereas the same peak arrives at FBG 2, at 1463.6 ms. The time difference, ΔT_{2-1}, is 0.4 ms. In the meantime, the peak of the waveform arrives at FBG 3 and FBG 4 at 1465.6 ms and 1466.2 ms, respectively. The time difference obtained for FBG 3 and FBG 4 (ΔT_{4-3}) is 0.6 ms. For 10 repetitions, the average time variation between ΔT_{2-1} and ΔT_{4-3} for no delamination is 0.04 ms (refer to Table 1).

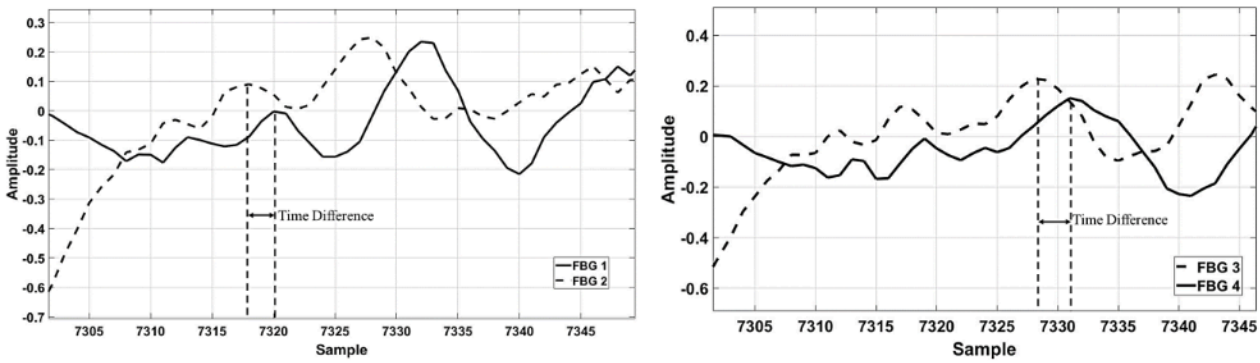

(a) (b)

Fig. 4. Signals captured for specimen without delamination (a) FBG 1 and FBG 2 (b) FBG 3 and FBG 4

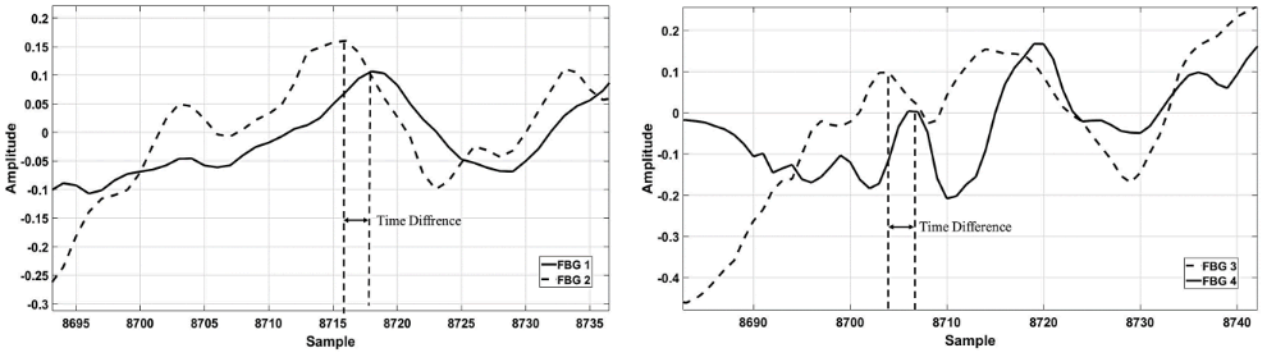

(a) (b)

Fig. 5. Signals captured for specimen with delamination 10 cm x 4 cm (a) FBG 1 and FBG 2 (b) FBG 3 and FBG 4

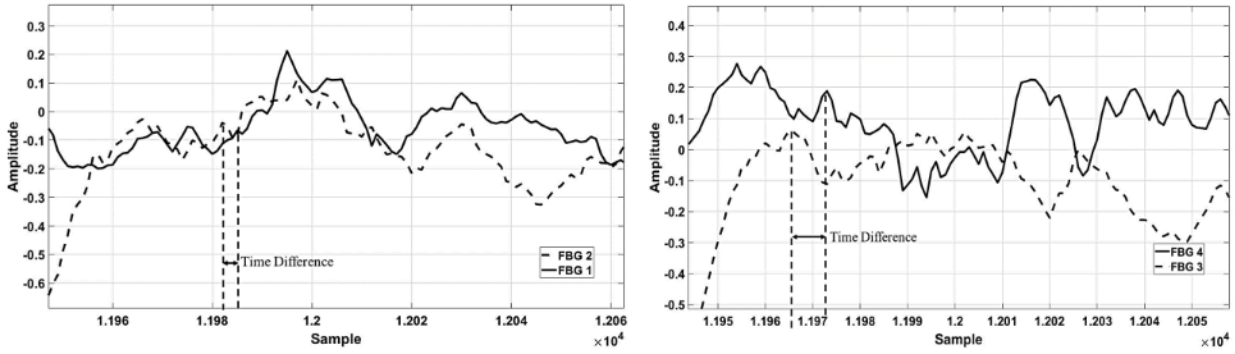

Fig. 6. Signals captured for specimen with delamination 10 cm x 6 cm (a) FBG 1 and FBG 2 (b) FBG 3 and FBG 4

Subsequently, it is observed that the presence of delamination has affected the time delay, which is different between ΔT_{2-1} and ΔT_{4-3}. For the delamination size of 10 cm × 4 cm (or 26.67% of the detection area), the average time difference between signals at FBG 3 and FBG 4 is recorded at 0.74 ms for 10 recurrences. While the waveform captured at FBG 1 and FBG 2 has an average time difference of 0.44 ms for 10 recurrences, as a result, the time delay between ΔT_{2-1} and ΔT_{4-3} for the delamination size of 10 cm × 4 cm increases significantly, with an average of 0.30 ms. In the meantime, for the specimen with a delamination area of 10 cm x 6 cm, the time delay increases significantly. The time difference between FBG 3 and FBG 4 ranged between 0.6 ms and 1.8 ms, with the average being 1.04 ms, for 10 replications. While the time differences for FBG 1 and FBG 2 ranged between 0.2 ms and 0.6 ms, with an average of 0.48 ms for 10 replications.

Table 1 shows a summary of the time delay for all delamination condition; without delamination, with the delamination area of 10 cm × 4 cm and 10 cm × 6 cm. The percentage of average time delay is determined from the average time different over the time different at FBG 1 and 2 (Eq. (5)). The results reveal that the existence of delamination will increase the time difference of the signals between two points of measurement. Similar results were also reported by Wang *et al.,* [32] and Rekatsinas *et al.,* [33]. This could be explained as the waves required to propagate through a larger air gap of delamination before reaching FBG 4.

$$\text{Time delay } \% = \frac{|\Delta T|}{\Delta T_{2-1}} \times 100 \tag{5}$$

Table 1
The average time delay for all delamination condition (10 repetitions)

Delamination size (%)	ΔT_{2-1}, (*ms*)	ΔT_{4-3}, (*ms*)	$\lvert\Delta T\rvert$ (*ms*)	Time delay (%)
0.0	0.38	0.34	0.04	10.5
26.7	0.44	0.74	0.30	68.2
40.0	0.48	1.04	0.56	116.7

3.2 Velocity Analysis

A velocity analysis is conducted in order to assess the magnitude of the wave velocity that propagated across the delamination region. Figure 7 illustrates the velocity of the signal, denoted as V_1 and V_2, which has been determined by calculating the time differences between FBG 1 and FBG 2, and FBG 3 and FBG 4, respectively. These calculations have been performed for three distinct regions: the specimen area without delamination, as well as the delamination areas of 10 cm × 4 cm and 10 cm × 6 cm, respectively. The average velocities of wave travel for a region without delamination were

determined to be 39.47 cm/ms for V_1 and 44.12 cm/ms for V_2, based on the known distance and time difference. In the context of the delamination region measuring 10 cm × 4 cm, the average velocities were determined to be 34.09 cm/ms for V_1 and 20.27 cm/ms for V_2. In contrast, the velocities for the delamination region of 10 cm x 6 cm were determined to be 31.25 cm/ms and 14.42 cm/ms for V_1 and V_2, respectively. The velocities for all delamination situations were summarised and organised in Table 2. The velocity analysis indicates that the specimens without delamination exhibit a high degree of similarity. This is evident from the small difference in the time it takes for the wave to travel from impact point to sensor FBG 1 and sensor FBG 2, as observed in the collected signal. Furthermore, the percentage variation in value on V_1 for the three specimens, namely the part without delamination, is barely 15.52%. This indicates that the sensor's placement whether in horizontal or vertical arrangement on the specimen does not impact the characteristics of the signal detected by the sensor.

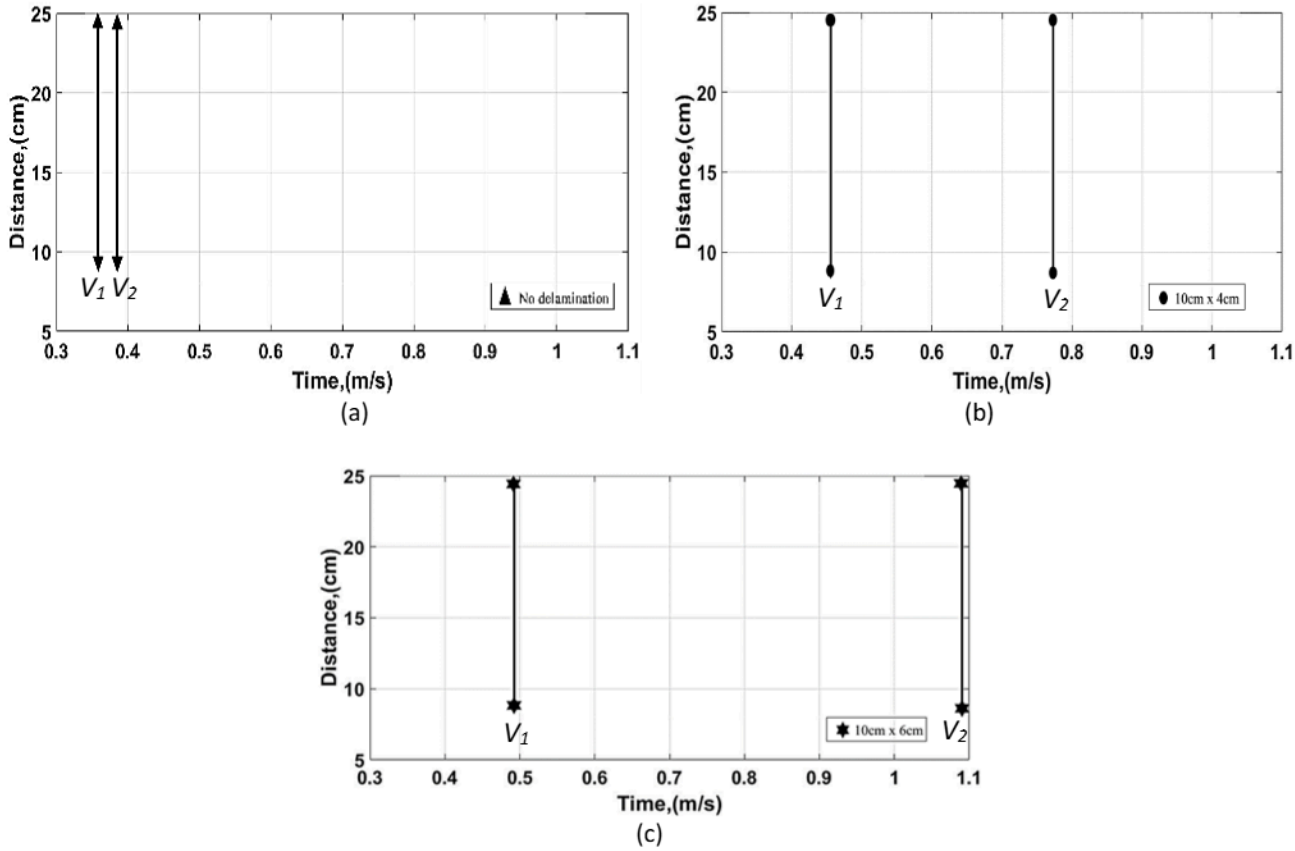

Fig. 7. The velocity response for three composites (a) No delamination (b) 10 cm x 4 cm (c) 10 cm x 6 cm

Table 2
The summary of velocity for all delamination conditions

Delamination size (%)	V_1, (cm/ms)	V_2, (cm/ms)	Velocity reduction, $V_1 - V_2$ (cm/ms)	Velocity reduction (%)
0.0	39.47	44.12	-4.65	-11.78
26.7	34.09	20.27	13.82	40.54
40.0	31.25	14.42	16.83	53.85

The tabulation presented in Figure 8 illustrates the recorded values of V_1 and V_2 for both areas devoid of delamination and those exhibiting delamination. The observed clusters of groups pertaining to V_1 and V_2 illustrate the dissimilarity in the deceleration of velocity due to the occurrence

of delamination. Moreover, it has been shown that the velocity of the wave tends to decrease as the size of the delamination grows. It was also noted that there exists a linear link between the percentage of delamination size, as indicated by Eq. (4), and the percentage of velocity decrease, with a high R-squared value of 0.98 as shown in Figure 9. To support this, the relationship between the velocity of the wave and the stiffness of the structure has been discussed by Murat *et al.,* [34]. The expansion of the delamination region resulted in a decrease in the structural stiffness, thereby leading to a reduction in the velocity of the waves. The increase in time delay is also related to the extended path length or scattering effects introduced by the delamination. Therefore, it can be concluded that the bonding of the composite between its layer and the material toughness plays a role in their ability to transmit waves or sustain loads. By interpreting these fitting parameters in the context of specific physical properties, the predictive accuracy and reliability of the FBG sensor network for delamination detection in composite structures can be improved.

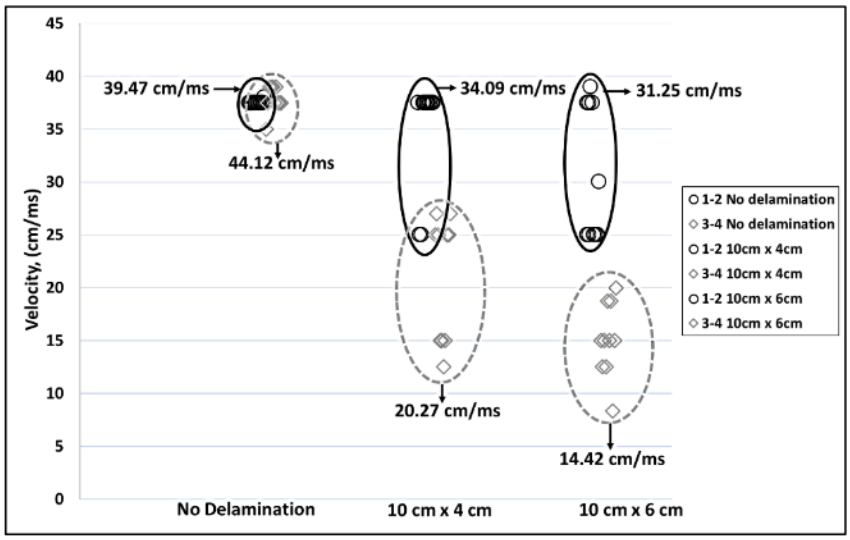

Fig. 8. Tabulation of of V_1 and V_2 for all trials

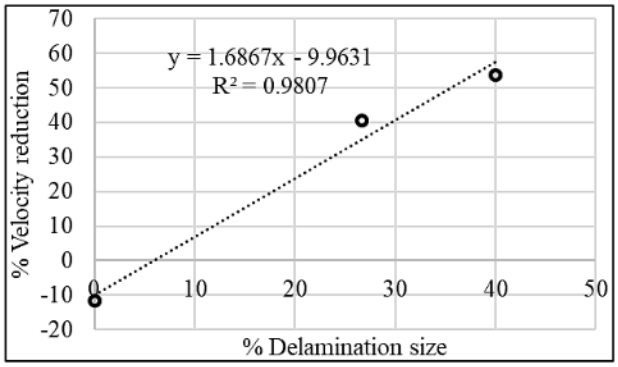

Fig. 9. Velocity reduction vs delamination size

4. Conclusions

This study examines acoustic wave analysis and FBG sensor network as methods for inspecting composite plates with delamination areas measuring 10 cm × 4 cm and 10 cm × 6 cm. A control region on the same specimen, devoid of any delamination, was utilised. The analysis focused on two acoustic factors, namely the time delay and velocity. The experimental findings unambiguously demonstrated a substantial variability in the parameters across varying delamination areas. The increase in

delamination size is directly proportional to the corresponding increase in time delay. Specifically, when the delamination area is 10 cm x 4 cm, the time delay is measured at 68.2%. Conversely, when the delamination area is 10 cm x 6 cm, the time delay is seen to be 116.7%. As a result, it can be shown that in the examination of velocity, an increase in the extent of delamination leads to a considerable reduction in wave speed. The wave speed was seen to fall by 40.54% for a delamination area of 10 cm x 4 cm, whereas a delamination area of 10 cm x 6 cm resulted in a velocity decrease of 53.85%. The observed decrease in speed is in accordance with the proportion of delamination area, suggesting a clear correlation between these two variables. The aforementioned findings provide convincing evidence that the utilization of a Fibre Bragg Grating (FBG) sensor network for delamination detection may indeed serve as a viable option for the purpose of health monitoring in plate-like composite structures.

Acknowledgement
This research received the financial support from Ministry of Higher Education Malaysia under the Fundamental Research Grant Scheme FRGS/1/2019/TK03/UMP/02/7 @ RDU1901116.

References

[1] Hsissou, Rachid, Rajaa Seghiri, Zakaria Benzekri, Miloudi Hilali, Mohamed Rafik, and Ahmed Elharfi. "Polymer composite materials: A comprehensive review." *Composite Structures* 262 (2021): 113640. https://doi.org/10.1016/j.compstruct.2021.113640

[2] Helaili, Sofiene, Moez Chafra, and Yvon Chevalier. "Alfa natural fiber composite reinforcement for concrete beams." *Civ Eng Archit* 9, no. 6 (2021): 1677-1686. https://doi.org/10.13189/cea.2021.090602

[3] Xu, Wei, Zhongqing Su, Jingqiang Liu, Maosen Cao, and Wiesław Ostachowicz. "Singular energy component for identification of initial delamination in CFRP laminates through piezoelectric actuation and non-contact measurement." *Smart Materials and Structures* 29, no. 4 (2020): 045001. https://doi.org/10.1088/1361-665X/ab6fe6

[4] uadrado, Manuel, Jesus Pernas-Sanchez, José Alfonso Artero-Guerrero, and David Varas. "Detection of barely visible multi-impact damage on carbon/epoxy composite plates using frequency response function correlation analysis." *Measurement* 196 (2022): 111194. https://doi.org/10.1016/j.measurement.2022.111194

[5] Derusova, D. A., V. P. Vavilov, V. Shpilnoi, A. O. Siddiqui, Y. L. V. D. Prasad, N. V. Druzhinin, and V. Yu Zhvyrblya. "Characterising hidden defects in GFRP/CFRP composites by using laser vibrometry and active IR thermography." *Nondestructive Testing and Evaluation* 37, no. 6 (2022): 776-794. https://doi.org/10.1080/10589759.2022.2063285

[6] Kasim, Mohd Shahir, W. Noor Fatihah W. Mohamad, Raja Izamshah, Noraiham Mohamad, Hairulhisham Rosnan, Syahrul Azwan Sundi, Muhammad Hafiz Hassan, Teruaki Ito, and Zamri Mat Kasa. "Analysis of carbon fiber-reinforced polymer composites delamination during vibration assisted trimming using historical data design." *Malaysian Journal on Composites Science and Manufacturing* 6, no. 1 (2021): 1-13.https://doi.org/10.37934/mjcsm.6.1.113

[7] Takeda, S., Y. Okabe, and N. Takeda. "Delamination detection in CFRP laminates with embedded small-diameter fiber Bragg grating sensors." *Composites Part A: Applied Science and Manufacturing* 33, no. 7 (2002): 971-980. https://doi.org/10.1016/S1359-835X(02)00036-2

[8] Dey, Nilanjan, Amira S. Ashour, Waleed S. Mohamed, Nhu Gia Nguyen, Nilanjan Dey, Amira S. Ashour, Waleed S. Mohamed, and Nhu Gia Nguyen. "Acoustic wave technology." *Acoustic Sensors for Biomedical Applications* (2019): 21-31. https://doi.org/10.1007/978-3-319-92225-6_3

[9] Alleyne, David N., and Peter Cawley. "The interaction of Lamb waves with defects." *IEEE Transactions On Ultrasonics, Ferroelectrics, and Frequency Control* 39, no. 3 (1992): 381-397. https://doi.org/10.1109/58.143172

[10] Gao, Fei, Lifu Wang, Jiadong Hua, Jing Lin, and Ajit Mal. "Application of Lamb wave and its coda waves to disbond detection in an aeronautical honeycomb composite sandwich." *Mechanical Systems and Signal Processing* 146 (2021): 107063. https://doi.org/10.1016/j.ymssp.2020.107063

[11] Jagadeeshwar, Tabjula L., Sheetal Kalyani, Prabhu Rajagopal, and Balaji Srinivasan. "Statistics-based baseline-free approach for rapid inspection of delamination in composite structures using ultrasonic guided waves." *Structural Health Monitoring* 21, no. 6 (2022): 2719-2731. https://doi.org/10.1177/14759217211073335

[12] Xu, Caibin, Zhibo Yang, Hao Zuo, and Mingxi Deng. "Minimum variance Lamb wave imaging based on weighted sparse decomposition coefficients in quasi-isotropic composite laminates." *Composite Structures* 275 (2021): 114432. https://doi.org/10.1016/j.compstruct.2021.114432
[13] Wang, Junzhen, and Yanfeng Shen. "Numerical investigation of ultrasonic guided wave dynamics in piezoelectric composite plates for establishing structural self-sensing." *Journal of Shanghai Jiaotong University (Science)* 23 (2018): 175-181. https://doi.org/10.1007/s12204-018-1923-z
[14] Zhao, Guoqi, Ben Wang, Tao Wang, Wenfeng Hao, and Ying Luo. "Detection and monitoring of delamination in composite laminates using ultrasonic guided wave." *Composite Structures* 225 (2019): 111161. https://doi.org/10.1016/j.compstruct.2019.111161
[15] Hervin, F., L. Maio, and P. Fromme. "Guided wave scattering at a delamination in a quasi-isotropic composite laminate: Experiment and simulation." *Composite Structures* 275 (2021): 114406. https://doi.org/10.1016/j.compstruct.2021.114406
[16] Aggelis, D. G., Sven De Sutter, Svetlana Verbruggen, Eleni Tsangouri, and Tine Tysmans. "Acoustic emission characterization of damage sources of lightweight hybrid concrete beams." *Engineering Fracture Mechanics* 210 (2019): 181-188. https://doi.org/10.1016/j.engfracmech.2018.04.019
[17] Li, Wei, Yinghonglin Liu, Peng Jiang, Fuping Guo, and Jiahao Cheng. "Study on delamination damage of CFRP laminates based on acoustic emission and micro visualization." *Materials* 15, no. 4 (2022): 1483. https://doi.org/10.3390/ma15041483
[18] Saeedifar, Milad, Mehdi Ahmadi Najafabadi, Dimitrios Zarouchas, Hossein Hosseini Toudeshky, and Meisam Jalalvand. "Barely visible impact damage assessment in laminated composites using acoustic emission." *Composites Part B: Engineering* 152 (2018): 180-192. https://doi.org/10.1016/j.compositesb.2018.07.016
[19] Ismail, N., Z. M. Hafizi, Cheong-Weng Ooi, Muhammad Khairol Annuar Bin Zaini, C. K. E. Nizwan, Kok-Sing Lim, and Harith Ahmad. "Fiber Bragg grating-based Fabry-Perot interferometer sensor for damage detection on thin aluminum plate." *IEEE Sensors Journal* 20, no. 7 (2019): 3564-3571. https://doi.org/10.1109/JSEN.2019.2959068
[20] Teixeira, João GV, Ivo T. Leite, Susana Silva, and Orlando Frazão. "Advanced fiber-optic acoustic sensors." *Photonic Sensors* 4 (2014): 198-208. https://doi.org/10.1007/s13320-014-0148-5
[21] Ameen, Odai Falah, Marwan Hafeedh Younus, RK Raja Ibrahim, and Rosly Abdul Rahman. "Comparison of water level measurement performance for two different types of diaphragm using fiber Bragg grating based optical sensors." *Jurnal Teknologi* 78, no. 6-11 (2016). https://doi.org/10.11113/jt.v78.9203
[22] Harun, Sulaiman Wadi, Prabakaran Poopalan, and Harith Ahmad. "Fabrication of fiber Bragg gratings in high germania boron co-doped optical fiber by the phase mask method." *Jurnal Teknologi* (2002): 11â-18.
[23] Salih, Younis Mohammed, Yusof Munajat, and Hazri Bakhtiar. "Response of fbgâ€"bonded plastic plate at different locations of applied stress." *Jurnal Teknologi* 78, no. 6-11 (2016). https://doi.org/10.11113/jt.v78.9201
[24] Austin, Timothy SP, Margaret M. Singh, Peter J. Gregson, John P. Dakin, and Philip M. Powell. "Damage assessment in hybrid laminates using an array of embedded fiber optic sensors." In *Smart Structures and Materials 1999: Smart Systems for Bridges, Structures, and Highways*, 3671, p. 281-288. SPIE, 1999. https://doi.org/10.1117/12.348677
[25] Leng, J. S., and A. Asundi. "Non-destructive evaluation of smart materials by using extrinsic Fabry–Perot interferometric and fiber Bragg grating sensors." *Ndt & E International* 35, no. 4 (2002): 273-276. https://doi.org/10.1016/S0963-8695(01)00060-3
[26] Takeda, Nobuo, Yoji Okabe, Ryohei Tsuji, and Shin-ichi Takeda. "Application of chirped fiber Bragg grating sensors for damage identification in composites." In *Smart Structures and Materials 2002: Smart Sensor Technology and Measurement Systems*, 4694, p. 106-117. SPIE, 2002. https://doi.org/10.1117/12.472608
[27] Takeda, S., S. Minakuchi, Y. Okabe, and N. Takeda. "Delamination monitoring of laminated composites subjected to low-velocity impact using small-diameter FBG sensors." *Composites Part A: Applied Science and Manufacturing* 36, no. 7 (2005): 903-908. https://doi.org/10.1016/j.compositesa.2004.12.005
[28] Ling, Hang-yin, Kin-tak Lau, Li Cheng, and Wei Jin. "Utilization of embedded optical fibre sensors for delamination characterization in composite laminates using a static strain method." *Smart Materials and Structures* 14, no. 6 (2005): 1377. https://doi.org/10.1088/0964-1726/14/6/030
[29] Takahashi, Nobuaki, Kanta Tetsumura, and Sumio Takahashi. "Underwater acoustic sensor using optical fiber Bragg grating as detecting element." *Japanese Journal of Applied Physics* 38, no. 5S (1999): 3233. https://doi.org/10.1143/JJAP.38.3233
[30] Gong, Zhe, Heming Wei, Zhangli Wu, Fufei Pang, Tingyun Wang, and Sridhar Krishnaswamy. "High-sensitive FBG-based adaptive fiber laser acoustic sensing system." In *AOPC 2021: Optical Sensing and Imaging Technology* 12065, p. 645-651. SPIE, 2021. https://doi.org/10.1117/12.2606754
[31] Sridhar, S., Suneetha Sebastian, Ajay K. Sood, and Sundarrajan Asokan. "A study on MoS_2 nanolayer coated etched fiber Bragg grating strain sensor." *IEEE Sensors Journal* 21, no. 7 (2021): 9171-9178. https://doi.org/10.1109/JSEN.2021.3054473

[32] Wang, Fei, Junyan Liu, Lixia Liu, Lixia Xu, Yonghui Wang, Mingjun Chen, and Yang Wang. "Quantitative non-destructive evaluation of CFRP delamination defect using laser induced chirp-pulsed radar photothermal tomography." *Optics and Lasers in Engineering* 149 (2022): 106830. https://doi.org/10.1016/j.optlaseng.2021.106830

[33] Rekatsinas, C. S., N. A. Chrysochoidis, and D. A. Saravanos. "Investigation of critical delamination characteristics in composite plates combining cubic spline piezo-layerwise mechanics and time domain spectral finite elements." *Wave Motion* 106 (2021): 102752. [34] Bibi IS Murat, Pouyan Khalili, and Paul Fromme. "Scattering of guided waves at delaminations in composite plates." *The Journal of the Acoustical Society of America* 139, no. 6 (2016): 3044-3052. https://doi.org/10.1016/j.wavemoti.2021.102752

[34] Bibi IS Murat, Pouyan Khalili, and Paul Fromme. "Scattering of guided waves at delaminations in composite plates." *The Journal of the Acoustical Society of America* 139, no. 6 (2016): 3044-3052. https://doi.org/10.1016/j.wavemoti.2021.102752